Magnet Temperature Estimation in Variable Leakage Flux Permanent Magnet Synchronous Machines Using the Magnet Flux Linkage

Diego F. Laborda
University of Oviedo
Dept. of Elect., Computer &
System Engineering
Gijón, Spain
dflaborda@uniovi.es

David Díaz Reigosa
University of Oviedo
Dept. of Elect., Computer &
System Engineering
Gijón, Spain
diazdavid@uniovi.es

Daniel Fernández
University of Oviedo
Dept. of Elect., Computer &
System Engineering
Gijón, Spain
fernandezalodaniel@uniovi.es

Kensuke Sasaki
Nissan Motor Co. Ltd
EV System Laboratory
Atsugi, Kanagawa, Japan
kensuke-sasaki@mail.nissan.co.jp

Takashi Kato
Nissan Motor Co. Ltd
EV System Laboratory
Atsugi, Kanagawa, Japan
katou-t@mail.nissan.co.jp

Fernando Briz
University of Oviedo
Dept. of Elect., Computer &
System Engineering
Gijón, Spain
fernando@isa.uniovi.es

Abstract—**Permanent magnet synchronous machines (PMSMs) performance is highly dependent on the Permanent Magnets (PMs) temperature. Knowledge of the PMs temperature is therefore of great importance both for control and monitoring purposes. An increase in the PM temperature during motor operation, decreases PMs magnetic flux strength and consequently the PMSM torque production capability, eventually causing irreversible demagnetization of the PMs; for the case of variable leakage flux PMSMs (VLF- PMSMs), it will affect the variable leakage property of the machine, which will place additional concerns on the machine control. This paper proposes a PM temperature estimation method for VLF-PMSMs from the PM flux linkage. PM flux linkage is obtained from the response of the machine to a small-amplitude, low frequency, square-wave signal (either voltage or current). The signal is injected on top of the fundamental excitation, allowing on-line temperature estimation without interfering with the operation of the machine**

Keywords— Permanent magnet, temperature estimation, Variable leakage flux machine, VLF- PMSMs, magnet flux linkage.

I. Introduction

Permanent Magnet Synchronous Motors (PMSMs) are the preferred option for electric and hybrid-electric vehicles (EV & HEV) due to their high torque density, wide speed capability, and higher efficiency. A concern for this type of machine is the need to inject negative d-axis current to counteract permanent magnet (PM) flux linkage when the drive operates at high speeds, to match the back electromotive force (Back-EMF) with the available DC voltage [1]. This operating mode is known as flux-weakening and is characterized by an inherent copper and core loss increase due to the continuous application of negative d-axis current and the extra harmonics produced in the airgap field [1]. Extra losses will reduce the efficiency, the associated temperature increase eventually affecting the life expectancy of the machine. Variable flux PMSMs (VF-PMSMs) [2] and variable leakage flux PMSMs (VLF-PMSMs) machine designs

[3] are aimed to reduce or even avoid the injection of flux weakening current and its subsequent adverse effects.

Independent of the PMSM design, magnet thermal monitoring is a major concern since an increase in the PM temperature results in a decrease of the PM strength which negatively impacts the torque production capability. Furthermore, excessive temperature can lead to irreversible demagnetization. The variation of the PM strength with temperature places additional concerns both in VF-PMSMs and VLF-PMSMs. In VF-PMSMs a variation of the PM strength will affect the magnetization/demagnetization process and torque control. In VLF-PMSMs a variation of the PM strength will affect the variable leakage property of the machine, eventually reducing the accuracy controlling torque. Knowledge of PM temperature can be useful for monitoring or torque control purposes, the accuracy requirements for the second being typically higher [4].

Direct measurement of PM temperature requires the use of rotor mounted sensors and slip rings or wireless transmission which penalizes the robustness and cost of the system. Alternatively, PM temperature can be estimated. PM temperature estimation methods can be roughly classified into thermal models [5][6], back-EMF based methods [6], and signal injection methods [7]–[9]. Thermal models require knowledge of stator and rotor geometry, materials and cooling system, which makes them highly dependent on the machine design. On the contrary, BEMF and signal injection methods do not require previous knowledge of the geometry and cooling system of the machine [6]–[9]. Both methods require the stator temperature to compensate for the stator resistance variation with temperature [6]–[9]. However, this is not a major drawback in principle, as the stator winding temperature is normally measured in standard machines by means of contact type sensors [6]–[9]. While signal injection methods can work in the whole speed range, back-

EMF based methods are not suitable for low speeds or standstill as the back-EMF is proportional to speed.

Already published signal injection methods [7]–[9] estimate the PM temperature from the variation of the machine high frequency resistance/inductance with PM temperature; these methods are sensitive to saturation and magnetoresistive effect [10]. On the contrary, the method proposed in this paper uses PM flux linkage variation with temperature. PM flux linkage can be obtained from the stator flux linkage, a small-amplitude, low frequency, square-wave voltage or current signal is injected in the stator windings for this purpose. The main advantage of the proposed method compared to [7]–[9] is that it does not rely on stator resistance or inductance changes with temperature, not being therefore affected by saturation nor magnetoresistive effect.

This paper is organized as follows: the proposed temperature estimation method based on PM flux linkage variation is presented in Section II; simulation results are shown in Section III; the test bench that will be used for experimental verification of the method is shown in IV; conclusions are finally provided in Section V.

II. TEMPERATURE ESTIMATION BASED ON PM FLUX LINKAGE VARIATION

This section describes the principles and implementation of the proposed temperature estimation method. PM flux linkage decreases as PM temperature increases [7]–[9],[11], meaning that PM flux linkage is a reliable metric for PM temperature. While this is an undesirable behavior since a decrease of the PM flux linkage reduces the machine torque production capability, it can be potentially used for PM temperature estimation purposes. PM flux linkage is the only responsible for back-EMF at no load, but it is hardly decoupled from stator flux linkage created by stator currents at loaded condition. In order to estimate the PM flux linkage, the method proposed in [12] is used. Fig. 1 shows both the torque/current control block diagram of a VLF-PMSMs and the proposed temperature estimation control block diagram, the main blocks being:

- Flux observer: estimates the stator flux linkage ($\hat{\lambda}_{sdq}^{r}$) from the measured stator current (i_{sdq}^{r}) and the commanded stator voltage (i.e. the output of the current regulator, v_{sdq}^{r*}).
- PM flux linkage estimator: it is estimated from the stator flux linkage provided by the flux observer, $\hat{\lambda}_{sdq}^{r}$, in combination with the response of the machine to a small-amplitude, low frequency, squarewave current that will be injected on top of the fundamental current (Δi_{sdq}^{r*}) [12].
- A look-up table (LUT) that links the estimated PM flux linkage and the PM temperature [13].

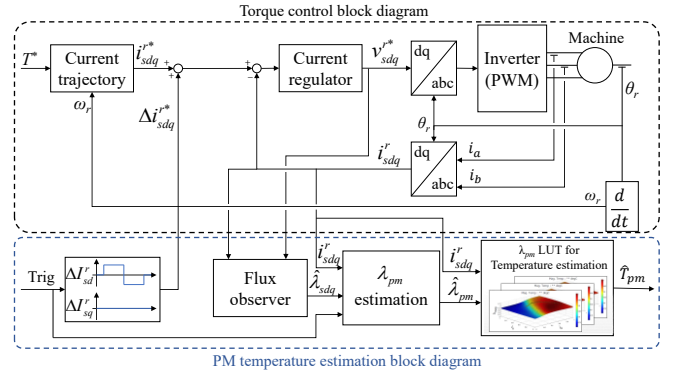All these blocks are described in detail following:

Fig. 1 – Temperature estimation system scheme.

A. Flux observer

Different stator flux observers have been proposed in the literature, the main types being voltage model [14][15], current model based [16] and Gopinath type [14]. Eq. (1) and (2) show the d and q-axis stator flux linkages as a function of stator d and q-axis voltages, currents and stator resistance, i.e. voltage model of a PMSM, where λ_{sd}^{s} and λ_{sq}^{s} are d and q-axis flux linkages in the stator reference frame, V_{sd}^{s} and V_{sq}^{s} are the d and q-axis stator voltages in the stator reference frame, I_{sd}^{s} and I_{sq}^{s} are the d and q-axis stator currents in the stator reference frame, and R_{s} is the stator resistance. Equations (3) and (4) show the d and q-axis stator flux linkages as a function of stator currents, inductances and magnet flux linkage, typically known as current model, where λ_{sd}^{r} and λ_{sq}^{r} are d and q-axis flux linkages in the rotor reference frame, I_{sd}^{r} and I_{sq}^{r} are the d and q-axis stator currents in the rotor reference frame, L_d and L_q are the d and q-axis inductances, and λ_{pm} is the magnet flux linkage. Finally, the voltage and current model can be combined in a Gopinath type flux observer [14]. The advantages and drawbacks of these three models can be seen in Table I.

$$\lambda_{sd}^{s}(t) = \int (V_{sd}^{s}(t) - R_{s} \cdot I_{sd}^{s}(t)) \cdot dt \qquad (1)$$

$$\lambda_{sq}^{s}(t) = \int (V_{sq}^{s}(t) - R_{s} \cdot I_{sq}^{s}(t)) \cdot dt \qquad (2)$$

$$\lambda_{sd}^{r} = I_{sd}^{r} L_d + \lambda_{pm} \qquad (3)$$

$$\lambda_{sq}^{r} = I_{sq}^{r} L_q \qquad (4)$$

TABLE I. ADVANTAGES AND DRAWBACKS OF FLUX MODELS

	CURRENT MODEL	VOLTAGE MODEL	GOPINATH
Parameter independency	✖	✖	✖
No initial state error	✔	✖	✔
Estimation in the whole speed range, including standstill	✔	✖	✔

The current model can be used to estimate stator flux in the whole speed range of the machine, but parameters, such as magnet flux linkage and inductances, must be previously known. On the other hand, voltage model can be used to estimate machine flux at high speeds [15], at low speeds it becomes inaccurate due to the diminishing magnitude of the Back-EMF with the speed and it cannot be used at standstill. In addition, as a pure integrator is required to estimate the flux, there is an initial

estimation error (integration constant) which needs to be compensated.

Gopinath type flux observers combine voltage (at high speed) and the current models (at low speed including standstill), a PI controller being used to make a smooth transition between models. The controller bandwidth will set the transition frequency from current to voltage model. This type of flux observer provides reliable estimation in the whole speed range of the machine, including standstill, being more sensitive to machine parameters at low speeds.

From the previous discussion, it is concluded that, although the current model and Gopinath type flux observers can be used in the whole speed range of the machine, the only model that contains information about the PM flux linkage is the voltage model (1)-(2). Therefore, a voltage model flux observer in stator reference frame will be used for PM temperature estimation in this paper.

Fig. 2 shows the implementation of the flux observed based on the voltage model (1)-(2). The estimated stator flux linkage in the stator reference frame, λ_{sdq}^s, is obtained from the (1)-(2) after applying a high pass filter (HPF) to avoid the infinite DC gain of the pure integrator. Adaptive phase and magnitude compensation of HPF effects have been implemented. The estimated stator flux linkage in the rotor reference frame, λ_{sdq}^r, is obtained by applying Park's transformation to the estimated stator flux linkage; a low pass filter (LPF) is finally used to eliminate high frequency harmonics of the stator flux linkage; i.e. only the fundamental component of the stator flux linkage will be used for temperature estimation.
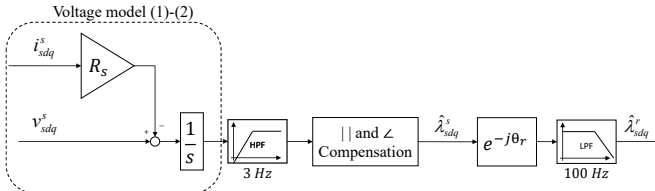

Fig. 2 – Voltage model flux observer in stationary reference frame.

B. PM flux linkage estimator

PM flux linkage is estimated from the stator flux linkage when a small-amplitude, low frequency, quasi-square wave current is added to the fundamental current [12][13]. The stator d-axis flux linkage response from the injected d-axis current will be used to estimate the PM flux linkage, as shown in Fig. 3.

The d-axis stator flux linkage, λ_{sd}^r, is represented by (5), λ_{sd}^{r+} is the d-axis flux linkage when positive d-axis current step, i.e. ΔI_{sd}^r, is applied (6), while λ_{sd}^{r-} is the d-axis flux linkage when negative d-axis current step, i.e. $-\Delta I_{sd}^r$, is applied (7). The stator flux linkages, λ_{sd}, λ_{sd}^{r+} and λ_{sd}^{r-} are estimated using the flux observer discussed in the previous subsection. $\hat{\lambda}_{pm}^+$ (estimated PM flux linkage when applying positive ΔI_{sd}^r) and $\hat{\lambda}_{pm}^-$ (estimated PM flux linkage when applying negative ΔI_{sd}^r)

are estimated from (8) and (9) respectively. Finally $\hat{\lambda}_{pm}$ is obtained as the average value of $\hat{\lambda}_{pm}^+$ and $\hat{\lambda}_{pm}^-$ in (10).

$$\lambda_{sd}^r = \lambda_{pm} + L_d \cdot I_{sd}^r \tag{5}$$

$$\lambda_{sd}^{r+} = \lambda_{pm}^+ + L_d^+ \cdot (I_{sd}^r + \Delta I_{sd}^r) \tag{6}$$

$$\lambda_{sd}^{r-} = \lambda_{pm}^- + L_d^- \cdot (I_{sd}^r - \Delta I_{sd}^r) \tag{7}$$

$$\hat{\lambda}_{pm}^+ = \frac{1}{\Delta I_{sd}} \left[I_{sd}^r \hat{\lambda}_{sd}^+ - (I_{sd}^r + \Delta I_{sd}^r) \hat{\lambda}_{sd} \right] \tag{8}$$

$$\hat{\lambda}_{pm}^- = \frac{1}{\Delta I_{sd}} \left[\left(I_{sd}^r - \Delta I_{sd}^r \right) \hat{\lambda}_{sd}^- - I_{sd}^r \hat{\lambda}_{sd} \right] \tag{9}$$

$$\hat{\lambda}_{pm} = \frac{\hat{\lambda}_{pm}^+ + \hat{\lambda}_{pm}^-}{2} \tag{10}$$
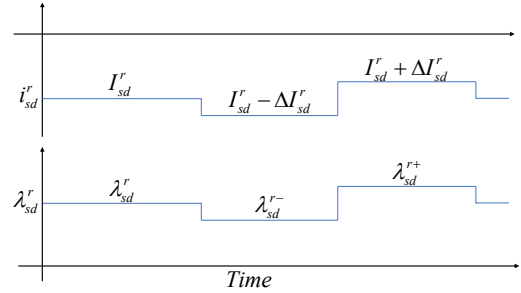

Fig. 3 – Schematic representation of the injected stator d-axis current, fundamental and small-amplitude, low frequency, squarewave currents, (i_{sd}^r) and resulting stator d-axis flux (λ_{sd}^r).

C. Temperature estimation

PM temperature estimation using PM flux linkage is especially challenging in VLF-PMSMs due to the variation of PM flux linkage with the stator current. Look-up tables (LUTs) will be used to compensate for this effect [13]. LUTs are built storing the estimated PM flux linkage ($\hat{\lambda}_{pm}$) values for different currents and PM temperatures. Linear interpolation is used to calculate PM temperature when the actual current or estimated PM value differs from stored values.

Fig. 4 shows an example of LUT which provides the PM flux linkage vs. stator current and PM temperature for the VLF-PMSMs test machine that will be used for the experimental verification of the method. It can be observed from Fig. 4 that the PM flux linkage decreases as the PM temperature (T_r) increases; this variation will be used for temperature estimation. It can be also observed that the PM flux linkage is heavily affected by stator current, which was an expected result due to the inherent variable leakage flux property of VLF-PMSMs.

Fig. 5 shows an example of the linear interpolation that has been performed to estimate the PM temperature when the d-axis is 0 A and the q-axis current is 400 A. The black dots in Fig. 5 are obtained from Fig. 4 at $I_{sd}^r = 0A$ and $I_{sq}^r = 400A$, a linear interpolation (blue line) being performed in this case.
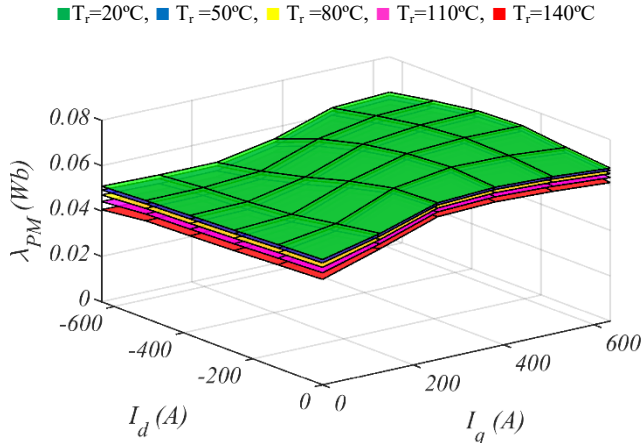
Fig. 4 – FEA results. PM flux linkage vs. stator current and PM temperature LUTs. w$_r$=3750 rpm, T$_r$=20, 50, 80, 110 and 140ºC.
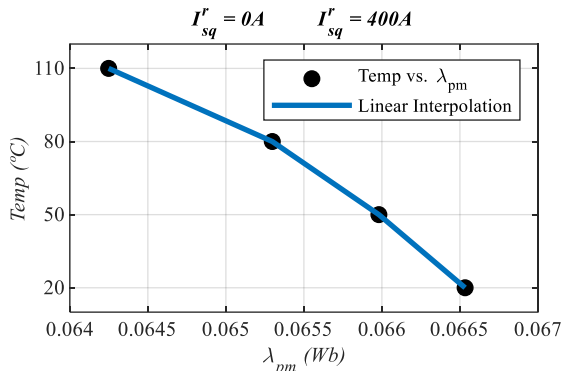

Fig. 5 – FEA results. Estimated PM flux linkage ($\hat{\lambda}_{pm}$) and linear interpolation for $I_{sd}^r = 0A$, $I_{sq}^r = 400A$ and T$_r$=20, 50, 80 and 110ºC.

III. SIMULATION RESULTS

Fig. 6 shows the schematic representation of the VLF-PMSMs that will be used both for simulation and experimental verification of the proposed method, the parameters being shown in Table II. The machine is a 110kW, 8 poles VLF-PMSM. Fig. 7a and 7b show the commanded d and q-axis currents, respectively, a square-wave current of $|\Delta I_{sd}^r|$=6.4 A (0.01 pu) being superposed to the fundamental d-axis current. Fig. 7c and 7d show the estimated stator d and q-axis flux linkage for different PM temperatures with the response to the currents shown in Fig. 7a and 7b; the stator flux linkages have been obtained using the flux observer described in Section II. Fig. 8 shows the estimated PM flux linkage, which is obtained from (6)-(10) after injecting a square-wave current signal, see Fig. 7a, at each fundamental dq-axis current level.

TABLE II. MACHINE PARAMETERS				
P$_{Rated}$ [kW]	I$_{Rated}$ [A]	ω_r [rpm]	T$_{Rated}$ [Nm]	Poles
110	640	10000	250	8

After the PM flux linkage is estimated, it is introduced in the stored LUTs to estimate temperature. During normal operation of the machine, the current operating point does not necessarily match with the stored values, in that case, interpolation of stored values must be performed. Linear and cubic spline interpolation methods are evaluated in this paper. Additionally, in order to

relate PM flux to temperature, the PM flux vs. temperature points must be interpolated in the stored LUTs. Linear and cubic spline interpolation methods are examined, and their performance is compared. It was found that quadratic regression of the PM flux vs. temperature provides accurate estimation, therefore it is also compared with interpolation methods.
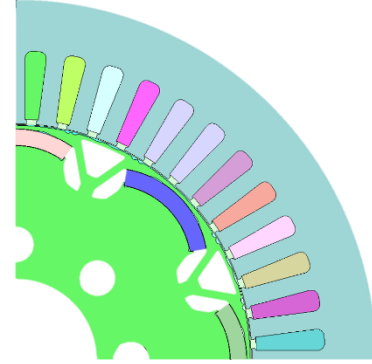

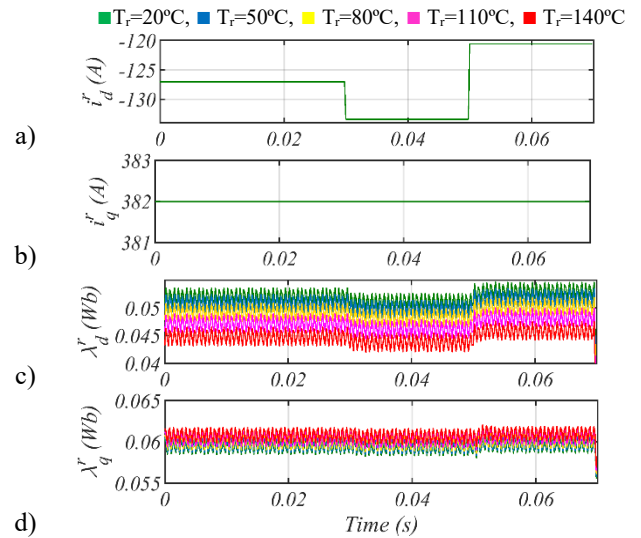Fig. 6 – Schematic representation of the test machine.

Fig. 7 – FEA results. a) d-axis and b) q-axis current c) estimated d-axis stator flux linkage and d) estimated q-axis stator flux linkage. $I_{sd}^r = -127A$, $I_{sq}^r = 382A$, ω_r=3750 rpm, T$_r$=20, 50, 80, 110 and 140ºC.
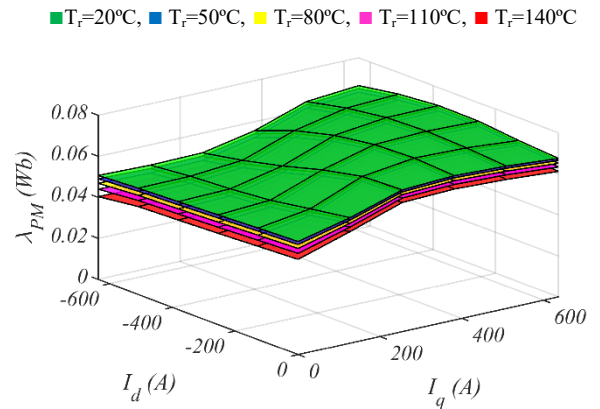
Fig. 8 – FEA results. Estimated PM flux linkage. ω_r=3750 rpm, T$_r$=20, 50, 80, 110 and 140ºC.

For operating point interpolation evaluation, new FEA simulations are performed at current levels different from the stored in the LUTs. Using the stored LUTs values, the PM flux at new simulated current levels is calculated through interpolations and compared with actual PM flux from FEA results at different temperatures (T_r=20, 50, 80, 110 and 140ºC). Fig. 9a and 9b show linear interpolation and cubic spline interpolation error, respectively. It is observed that, for this VLF-PMSM, the interpolation error is similar in both cases, therefore linear interpolation is preferred because it is computationally faster.

■T_r=20ºC, ■T_r=50ºC, ■T_r=80ºC, ■T_r=110ºC, ■T_r=140ºC

a)

b)
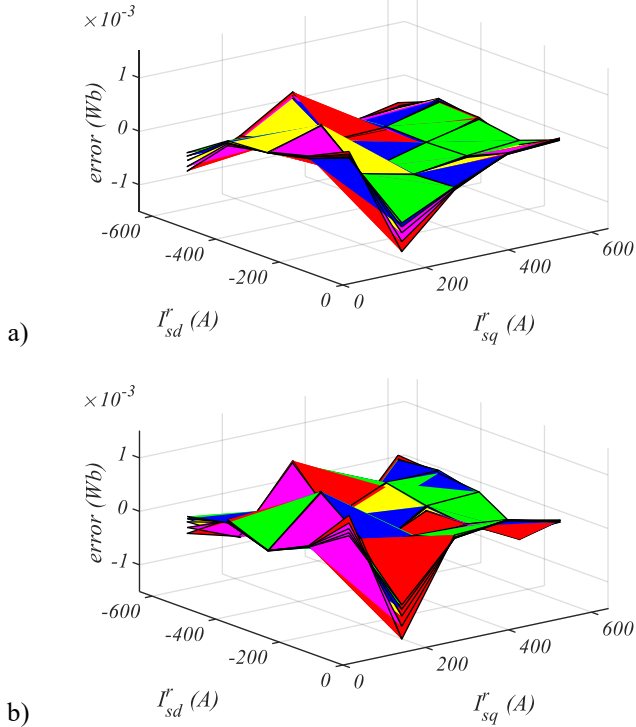
Fig. 9 – FEA results. a) introduced error by linear interpolation vs. stator current and b) introduced error by cubic spline interpolation vs. stator current. ω_r =3750 rpm, T_r=20, 50, 80, 110 and 140ºC

For PM flux vs. temperature interpolation, it is not possible to perform additional FEA simulations at other temperatures because the PM material behavior is only defined at 20, 50, 80, 110 and 140ºC, therefore T_r=80ºC is removed from interpolation and selected as test point. Fig. 10 shows linear, cubic spline interpolations and quadratic regression performed at zero stator current operating point. Their performance is compared using the actual PM flux linkage from FEA results at 80ºC, and PM temperature is obtained using proposed interpolations and regression. Fig. 11 shows the temperature estimation error that these interpolations introduce in the temperature estimation method at 80ºC. It is observed that cubic spline interpolation has very good accuracy, while the linear interpolation method exhibits larger error. Quadratic regression shows slightly worse accuracy than cubic spline interpolation but at a lower

computational cost. For final temperature estimation results, the linear interpolation accuracy is considered acceptable.
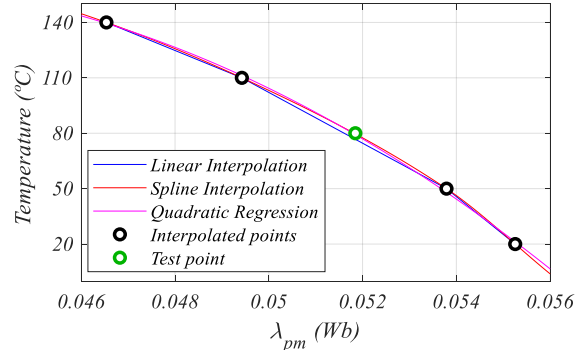

Fig. 10 – FEA results. Actual PM flux linkage ($\dot{\lambda}_{pm}$) vs. PM temperature and interpolations for $I_{sd}^r = 0A$, $I_{sq}^r = 0A$ and T_r=20, 50, 80, 110 and 140ºC.

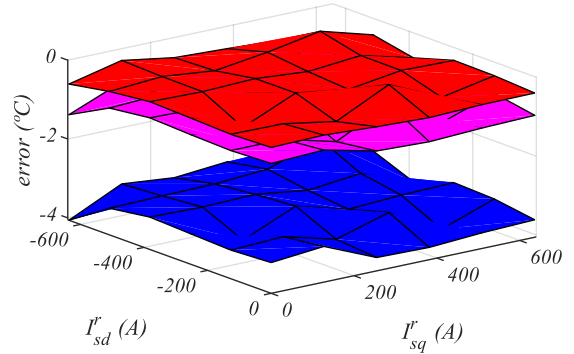■Linear Interpolation, ■Spline Interpolation, ■Quadratic Regression

Fig. 11 – FEA results. Introduced temperature estimation error by PM flux interpolations vs. stator current at T_r=80ºC and ω_r =3750 rpm

Finally, using the estimated PM flux linkage and stored LUTs, the PM temperature is estimated. Fig. 12 shows the estimated temperature and the estimation error, which is seen to be within 10ºC. This error can be considered adequate for demagnetization prevention purposes but might be excessive for precise torque control purposes.

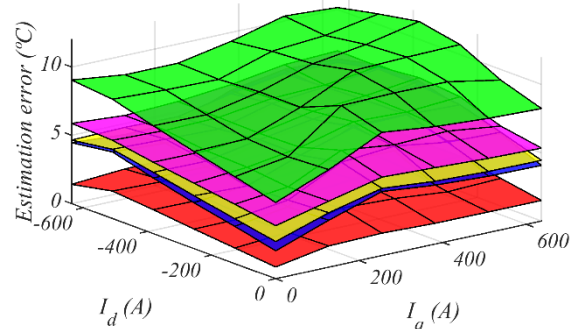■T_r=20ºC, ■T_r=50ºC, ■T_r=80ºC, ■T_r=110ºC, ■T_r=140ºC

Fig. 12 – FEA results. Temperature estimation error. ω_r =3750 rpm, T_r=20, 50, 80, 110 and 140ºC.

IV. EXPERIMENTAL SETUP AND RESULTS

A. Experimental setup

The test bench used for the experimental verification of the method can be seen in Fig. 13. The test bench is composed of a conventional IPMSM used as a load, the VLF-PMSM under test (parameters shown in Table II). Fig. 14 shows a schematic representation of the power system setup, where each machine is driven by a three-phase inverter with shared DC-link. The inverters are controlled using a TMS320F28335 microcontroller. Fig. 15 shows the control box with the control PCB and auxiliary systems.
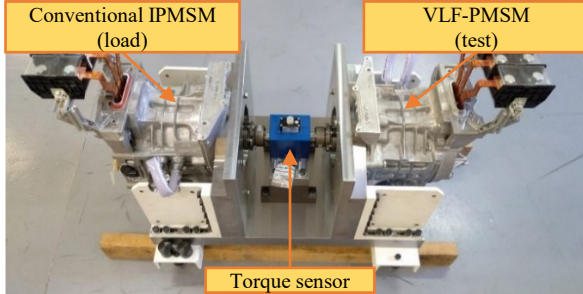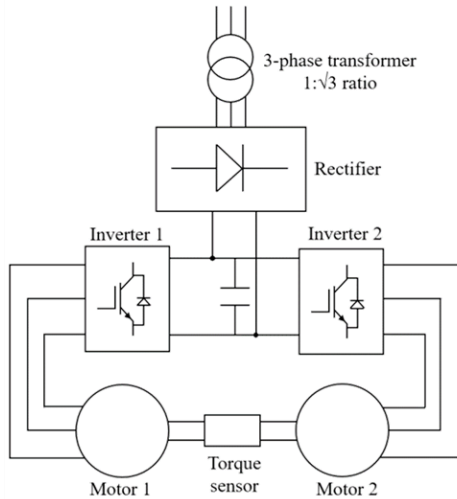

Fig. 13 – Test bench.
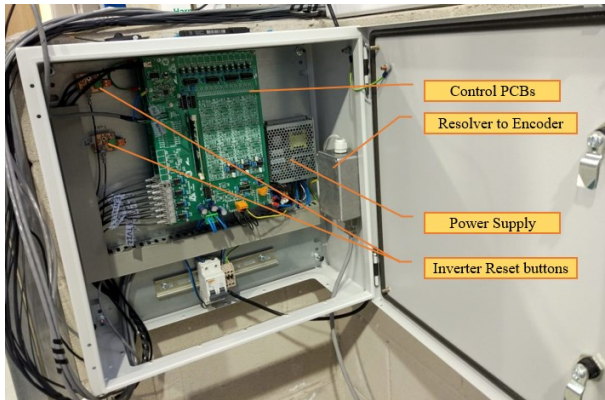

Fig. 14 – Experimental setup power system scheme.

Fig. 15 – Control box with the control card and auxiliary systems.

In order to verify the accuracy of the proposed PM estimation method, the rotor PMs temperature is measured by means of thermocouples. A wireless PM temperature measurement system has been developed and implemented to transmit the measured PM temperature to a PC that will collect the PMs temperatures. Fig. 16 shows a picture of the wireless PM temperature measurement system along with the aluminum case attached to the rear part of the rotor. The temperature measurement system includes all analog signal conditioning, anti-aliasing filters, a microcontroller with a 10-bit analog to digital converters and a Wi-Fi transmission module. One single-cell LiPo battery is used to deliver power to the whole measurement system.
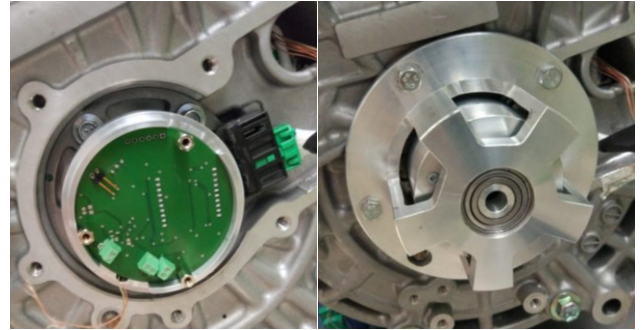

Fig. 16 – Wireless PM temperature measurement system along with the aluminum case attached to the rear part of the rotor.

B. Experimental results

First, the PM flux linkage of test machine is obtained with the stator flux observer and PM flux linkage estimation method presented in Section II at different temperatures (T_r=20, 50, 80 and 110ºC). Fig. 17 shows the online estimated PM flux linkage along with the FEA results at 20ºC for comparison. Experimental results exhibit lower PM flux linkage than FEA results, this is due to slightly lower magnetization of the PMs in the actual test machine. Despite this offset in the experimental results, the variable leakage flux capability can be observed, where the PM flux linkage increases at high load conditions (high q-axis current). It can be observed from Fig. 17 that experimental results have been performed up to 450 A, this was due to stator temperature limitations. The results shown in Fig. 17 will be stored in the microcontroller memory for PM temperature estimation during machine normal operation.

Fig. 18 shows the experimental results of the proposed PM temperature estimation method. Fig. 18a shows the d and q-axis currents that have been injected, Fig. 18b shows the estimated and measured temperatures and Fig. 18c shows the temperature estimation error. It can be observed that the temperature estimation error is <5ºC, what can be considered adequate for PM temperature monitoring applications.
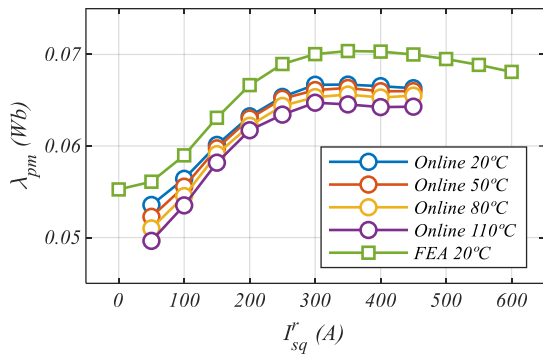
Fig. 17 – Experimental results. Estimated PM flux linkage and FEA results vs. q-axis stator current. $I_{sd}^r = -100A$, ω_r =3000 rpm, T_r=20, 50, 80 and 110ºC.
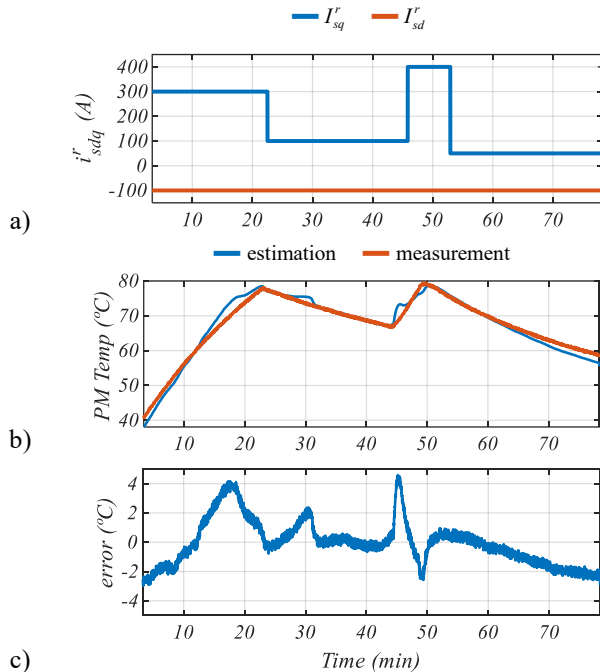

a)

b)

c)

Fig. 18 – Experimental results. a) d and q-axis current used during the experiment, b) Estimated and measured rotor PM temperature, c) estimation error.

V. CONCLUSIONS

This paper proposes a method for PM temperature estimation in VLF-PMSMs based on the PM flux linkage variation with temperature. PM flux linkage is obtained from the stator flux linkage of the machine after applying a small-amplitude, low frequency, square wave current signal, which is superposed on top of the fundamental current excitation. The method requires LUTs linking the PM flux linkage vs. stator current and PM temperature. Simulation and experimental results have been provided to demonstrate the validity of the proposed technique. The accuracy of the proposed method has been verified by using a wireless PM temperature measurement system.

REFERENCES

[1] Jang-Mok Kim and Seung-Ki Sul, "Speed control of interior permanent magnet synchronous motor drive for the flux weakening operation", IEEE Trans. Ind. Appl., 33(1): 43–48, Jan. 1997.

[2] V. Ostovic, "Memory motors", IEEE Ind. Appl. Mag., 9(1): 52–61, Jan. 2003.

[3] A. Athavale, T. Fukushige, T. Kato, C. Yu, and R. D. Lorenz, "Variable Leakage Flux IPMSMs for Reduced Losses Over a Driving Cycle While Maintaining Suitable Attributes for High-Frequency Injection-Based Rotor Position Self-Sensing", IEEE Trans. Ind. Appl., 52(1): 234–241, Jan. 2016.

[4] S. Li, B. Sarlioglu, S. Jurkovic, N. R. Patel, and P. Savagian, "Comparative Analysis of Torque Compensation Control Algorithms of Interior Permanent Magnet Machines for Automotive Applications Considering the Effects of Temperature Variation", IEEE Trans. Transp. Electrification, 3(3): 668–681, Sep. 2017.

[5] A. M. EL-Refaie, N. C. Harris, T. M. Jahns, and K. M. Rahman, "Thermal analysis of multibarrier interior PM synchronous Machine using lumped parameter model", IEEE Trans. Energy Convers., 19(2): 303–309, Jun. 2004.

[6] C. Kral, A. Haumer, and S. B. Lee, "A Practical Thermal Model for the Estimation of Permanent Magnet and Stator Winding Temperatures", IEEE Trans. Power Electron., 29(1): 455–464, Jan. 2014.

[7] D. D. Reigosa, D. Fernandez, H. Yoshida, T. Kato, and F. Briz, "Permanent-Magnet Temperature Estimation in PMSMs Using Pulsating High-Frequency Current Injection", IEEE Trans. Ind. Appl., 51(4): 3159–3168, Jul. 2015.

[8] D. D. Reigosa, F. Briz, P. Garcia, J. M. Guerrero, and M. W. Degner, "Magnet Temperature Estimation in Surface PM Machines Using High-Frequency Signal Injection", IEEE Trans. Ind. Appl., 46(4): 1468–1475, Jul. 2010.

[9] M. Ganchev, C. Kral, and T. Wolbank, "Sensorless rotor temperature estimation of permanent magnet synchronous motor under load conditions", in Conf. IEEE Ind. Electron. Soc., 2012, pp: 1999–2004.

[10] D. Fernandez, D. Reigosa, J. M. Guerrero, Z. Q. Zhu, C. Suarez, and F. Briz, "Influence of PM Coating on PM Magnetization State Estimation Methods Based on Magnetoresistive Effect", IEEE Trans. Ind. Appl., 54(3): 2141–2150, May 2018.

[11] D. Reigosa, D. Fernandez, T. Tanimoto, T. Kato, and F. Briz, "Comparative Analysis of BEMF and Pulsating High-Frequency Current Injection Methods for PM Temperature Estimation in PMSMs", IEEE Trans. Power Electron., 32(5): 3691–3699, May 2017.

[12] T. Kato, T. Matsuura, K. Sasaki, and T. Tanimoto, "Principle of variable leakage flux IPMSM using arc-shaped magnet considering variable motor parameter characteristics depending on load current", in Proc IEEE Energy Convers Congr Expo, 2017, pp: 5803–5810.

[13] T. Kato, K. Sasaki, D. F. Laborda, D. Fernández, D. Reigosa, "Magnet temperature estimation methodology by using magnet flux linkage observer for variable leakage flux IPMSM", IEEJ Journal of Industry Applications, 140(4): 265-271. Apr. 2020.

[14] P. L. Jansen and R. D. Lorenz, "A physically insightful approach to the design and accuracy assessment of flux observers for field oriented induction machine drives", IEEE Trans. Ind. Appl., 30(1): 101–110, Jan. 1994.

[15] J. S. Lee, C.-H. Choi, J.-K. Seok, and R. D. Lorenz, "Deadbeat-Direct Torque and Flux Control of Interior Permanent Magnet Synchronous Machines With Discrete Time Stator Current and Stator Flux Linkage Observer", IEEE Trans. Ind. Appl., 47(4): 1749–1758, Jul. 2011.

[16] H. Rehman, A. Derdiyok, M. K. Guven, and Longya Xu, "A new current model flux observer for wide speed range sensorless control of an induction machine", IEEE Trans. Power Electron., 17(6): 1041–1048, Nov. 2002.